



**HAL**  
open science

# Modeling and Measuring of Relative Motion at Contact Point of Electrical Connector for the Prediction of Vibration-Induced Fretting Damage

Mack Mavuni Nzamba, Erwann Carvou, Laurent Morin

► **To cite this version:**

Mack Mavuni Nzamba, Erwann Carvou, Laurent Morin. Modeling and Measuring of Relative Motion at Contact Point of Electrical Connector for the Prediction of Vibration-Induced Fretting Damage. IEEE Transactions on Components, Packaging and Manufacturing Technology, 2023, 13 (4), pp.489-501. 10.1109/TCPMT.2023.3272575 . hal-04148994

**HAL Id: hal-04148994**

**<https://hal.science/hal-04148994>**

Submitted on 5 Jul 2023

**HAL** is a multi-disciplinary open access archive for the deposit and dissemination of scientific research documents, whether they are published or not. The documents may come from teaching and research institutions in France or abroad, or from public or private research centers.

L'archive ouverte pluridisciplinaire **HAL**, est destinée au dépôt et à la diffusion de documents scientifiques de niveau recherche, publiés ou non, émanant des établissements d'enseignement et de recherche français ou étrangers, des laboratoires publics ou privés.



Distributed under a Creative Commons Attribution - NonCommercial 4.0 International License

# Modeling and measuring of relative motion at contact point of electrical connector for the prediction of vibration-induced fretting damage

Mack Mavuni Nzamba, Erwann Carvou, Laurent Morin

**Abstract**— The relative motion at the contact interface induced by engine vibration is one of the most significant causes for the fretting damage. However, at present, several vibration simulations models have been investigated in literature to predict fretting degradation. Unfortunately, those finite element (FE) models do not take into account all the connector components (more than 10) with the cable, the non-linear mechanical contact and the prestress state of different components after assembled process. This paper describes and illustrates the approaches used for a three-dimensional FE modeling and vibration simulation of electrical connector to evaluate the relative displacement between the terminals at contact point, and when the fretting occurs. A series of experimental tests were also conducted to validate the simulation. A sinusoidal vibration with a single frequency and amplitude were applied to the connector system. It was demonstrated that, test and simulation presented similar results. Finally, an approach for predicting connector risk of fretting damage is established by combining the contacts endurance and relative motion at contact point and eventually quantify the threshold amplitude of fretting.

**Index Terms**—Automotive, electrical connector, fretting, FE modeling, lifetime prediction, silver coating, vibration.

## NOMENCLATURE

SYMBOL	QUANTITY	UNITS
$f$	Vibration frequency.	Hz
$M$	Magnitude ratio, defined as $M_2/M_1$ .	
$M_1$	Magnitude of periodical motion of the female part of connector.	$\mu\text{m}$
$M_2$	Magnitude of periodical motion of the male part of connector.	$\mu\text{m}$
$R_c$	Electrical contact resistance (ECR).	$\text{m}\Omega$
$\Delta R_c$	Mean value of ECR under vibration subtracted by original value of ECR.	$\text{m}\Omega$

This work was supported in part by the ANRT and Aptiv company via Implementation Doctorate Programme. The authors gratefully acknowledge Mr. Konrad Kloch for his help with finites elements simulation.

M. Mavuni Nzamba is with the Department of Sciences Technology, University of Nouveaux Horizons, Lubumbashi, Congo (DRC) (e-mail: mack.mavuni@unhorizons.org)

E. Carvou is with the Institut de Physique de Rennes, University of Rennes, France (e-mail : erwann.carvou@univ-rennes1.fr).

L. Morin is with APTIV Compagny, Epernon, France (e-mail: laurent.morin@aptiv.com).

$U_1$	A function representing the periodic motion of the female part of connector.	
$U_2$	A function representing the periodic motion of the male part of connector.	
$\psi$	Phase difference, defined as $\psi_2 - \psi_1$ .	degree (°)
$\psi_1$	Phase of periodical motion of the female part of connector ( $U_1$ ).	degree (°)
$\psi_2$	Phase of periodical motion of the male part of connector ( $U_2$ ).	degree (°)
$\delta_{Limit}$	Threshold displacement amplitude.	$\mu\text{m}$
$(\Delta\delta_{ij})$	The maximum relative displacement defined as $ U_2 - U_1 $ .	$\mu\text{m}$
$\Delta\delta_t$	Relative displacement in total direction	$\mu\text{m}$
$\delta^*$	Displacement amplitude.	$\mu\text{m}$
$a_m$	Acceleration amplitude.	G ( $1G = 9.8 \text{ m/s}^2$ )
$E_t$	Tensile Young modulus.	GPa
$E_f$	Bending Young modulus.	GPa
$\nu_t$	Primary Poisson's ratios.	
$\nu_f$	Secondary Poisson's ratios.	

## I. INTRODUCTION

All the vehicles include several thousand electrical contact points distributed over several hundred connectors. The number of electrical connectors has grown steadily since the early days of the automotive, aeronautic, defense systems, etc. And the trend continues due to the ever-growing need for on-board electronics, sensors, and communication. Each faulty point of contact, among the thousands of on-board contacts, being a source of vehicle breakdown, so that the reliability of the connections is an essential point of customer satisfaction. With the foreseeable emergence of electric vehicles, reliability will also become a major safety issue. Beyond quality issues, one of the main types of connector failure are the wear and the oxidation of the contact points due to engine vibration and the environment conditions.

The physical phenomenon leading to this degradation is called "fretting corrosion". This is the wear and oxidation of the surfaces at the interface of the two members of the electrical contact when submitted to repeated relative displacements of a few micrometers [1- 4]. Actually, the qualification of connectors with respect to vibrations is mainly done on empirical basis of design rules. On the one hand, we know which design elements of the connector (electrical terminals, housings, connection of wires, etc.) and which coating materials make it possible to increase the resistance to vibration [3]. On the other hand, we do not have a tool to predict the lifespan of an interconnection system subjected to a given vibration profile. The development of a connector therefore goes through a phase of optimization loops based on tests results on a vibration bench test. Furthermore, each car

manufacturer having established its own test standards, it is sometimes difficult to guarantee that a connector can meet the specifications of two different manufacturers [5], [6], [7].

C. Chen *et al.* in 2009, modeled by finite elements the dynamic behavior of electrical connector subjected to vibrations. The same authors have compared the accuracy of using the three- and two-dimensional connector models [8]. Compared to the two-dimensional model, the three-dimensional model requires considerably more elements and larger computation resources, but provides more details of the model structure and dynamic behavior. The way vibrations cause contact micro-displacements (and eventual failures) depend on the connector parts assembly and their interactions. Varenberg *et al.* proposed a methodology for characterizing fretting in terms of the local relative motion [9]. In 2010, Ibrahim *et al.* [10], developed a FE model of blade-receptacle connector system with ABAQUS to simulate both induced vibrations and temperature in order to predict degradation by fretting corrosion.

Another environmental factor that influences electrical connector degradation is humidity. The corrosion of automotive connectors can be accelerated by humidity in vehicles [11] and the impact of humidity varies greatly for different type of coating materials [12], [13]. Dijk *et al.* [14] found that gold and silver are the best candidates since they have the lowest electrical resistance increase under fretting and humidity conditions. Zang *et al.* [15] proposed a 3-D model of electrical connector with the cable being taken into account. Indeed, Mashimo and *al.* [16] performed FE simulation on electrical connector and they emphasized the importance of taking into account the damping characteristic assigned to the cable when we modeled it.

In a recent study, Mavuni and Carvou [17] show that when the connector is submitted to vibration, the motions are transferred from the cable to the terminals. A chosen damping factor can either attenuate or amplify the movements of a mechanical system, dissipating the energy generated. Yaya and Miled [18], in their work, propose an approach to model the impact of ultrasonic welding on electrical contacts. They have included in the FE model the prestressed state of the electrical contacts resulting from the assembly of the components. This consideration of the prestressed state makes it possible to approximate the actual physical conditions of electrical contacts after assembly.

The present paper proposes a FE 3-D model of electrical connector which considers all the parts assembly (more than 10 parts) and the nonlinear mechanical behavior of contacts between different connector components. The FE simulation proposed is only mechanical i.e. only the vibration mechanical parameters were used as input. The created model is able to capture the micro displacement at contact interface, then compared it with the test results, as will be discussed later. Many works report that the degradation of the contact interface will lead the electrical contact resistance (ECR) to increase significantly with a sudden failure after a certain number of vibration cycles [19]–[20]. Carvou and Ben Jemaa explained that the contact surface moves along the track formed by oxide particles and as a result ECR varies periodically under vibration [21]. Fouvry *et al.* [4] studied the performance of an electrical contact in terms of electrical

endurance which is considered to be the number of cycles required to achieve a given contact resistance threshold. Indeed, the influence of the vibration amplitude was studied by Bouzera *et al.* [1]. They demonstrated that there is a minimum fretting amplitude such that below this value no degradation of the contact resistance is observed. Pompanon *et al.* [22] demonstrated that the amplitude of the transition between the partial and gross slip regimes depends on the contact force.

The vibration response of a system submitted to dynamic excitation depends on the one hand, on this vibration source (sinusoidal, random, frequency, amplitude, etc.) and, on the other hand on the geometry and the mass of this mechanical system. Therefore, many parameters must be taken into consideration. In the context of a connector, the connection between the male part (pin holder) and the female part (clip holder) is not glued. Hence, there are multiple degrees of freedom's motions. The vibratory response of the clip holder depends not only on its characteristics but also on the type of connection with the pin holder. Thus, the transmission of vibrations is complex and specific to each type of connector.

Thus, the aim of this study is to develop a vibration simulation model of connector, which allows quantifying the relative motions at contact point, in order to predict the risk of degradation during the early stage of design. In this study, the connector behavior was observed at different excitation conditions through the analysis of terminals and the cable motions. In order to confirm the validity of the simulation computed results, they were compared with those measured by experimental tests.

In previous study [17] we proposed a FE modal analysis methodology that allows us to detect the resonance frequency with a finite element method (FEM). Regarding this present study, the investigation of relative motion was done under non-resonate frequencies. The sinusoidal vibration was applied to the connector system with fixed frequency and amplitude. The response of such connectors under external vibration excitation was quantified by FE modeling and simulation first, then compared with experimental test results. In this paper, the electrical performances of the terminals are investigated in order to determine the threshold amplitude of fretting. The relative motion was compared to the minimum amplitude in order to predict the risk of fretting degradation. This work showed that the silver-to-silver contact has the lowest ECR increase after 24h of vibration test. Finally, the analysis of worn surfaces demonstrates that wear exists on silver-plated connectors, but no obvious fretting corrosion and oxidation build-up is detected. It is the relatively stable property of silver and also connector design that allows to get those good performances under vibration. Fu *et al.* [23] found the similar results by investigating a silver-plated high power connector performance under vibration.

The framework for connector fretting degradation prediction based on FE simulation and testing results after vibration was proposed in this paper, as shown in Fig. 1. This methodology proposed allows to predict the risk of fretting degradation i.e. the variation of the ECR in the real automotive electrical connectors.

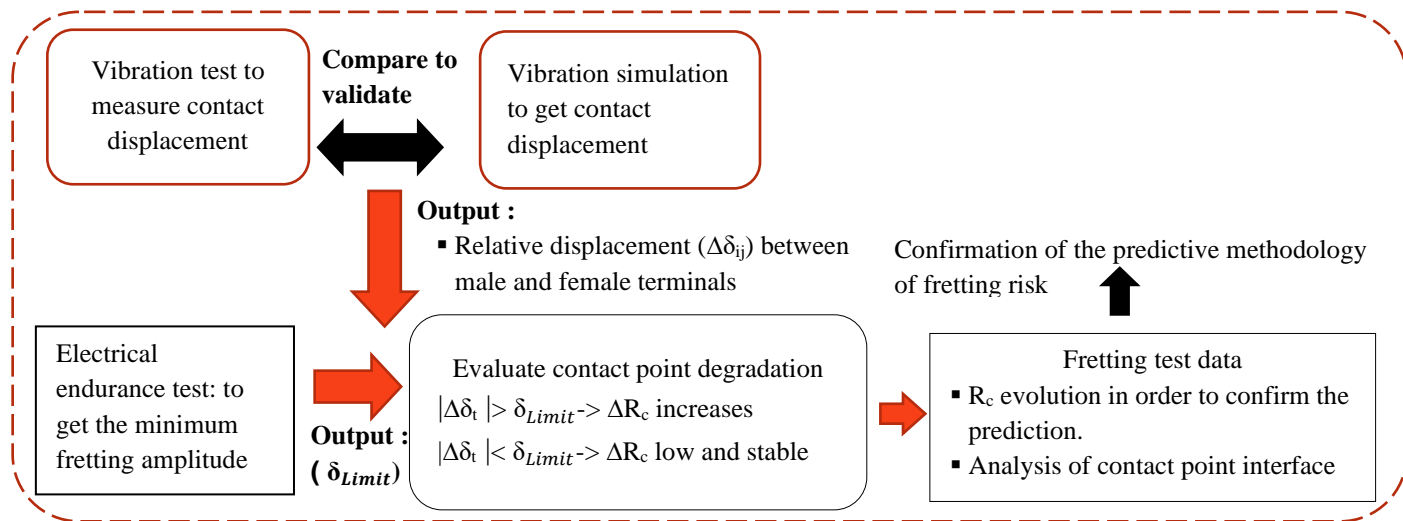


Fig. 1. Framework of the prediction methodology

## II. INTRODUCTION TO THE ELECTRICAL CONNECTOR

The connectors tested are 1-way automotive connectors manufactured by Aptiv. It's a high-power connector used in engine environments. The connector is able to work under current as high as 200 A, but the actual current applied in testing vibration is around 100 mA due to the automotive manufacturer standards. This connector consists of 11 parts where the main ones are insulating housings, contact pair (pin and clip) and spring lock, as shown in Fig. 2 (a), (b). The female part consists of twelve contact points symmetrically distributed (Fig.2 (c)). The wire, with 35 mm<sup>2</sup> of cross-section, is connected to the female part by ultrasonic welding. There are silicon parts which help to absorb vibration applied on the connector system. The electrical contact surface is plated with silver and the substrate connector material is copper, on which an electrolytic nickel interlayer was deposited in order to limit copper diffusion and the formation of intermetallic phases. Several works report that a connector with silver-plating coatings could make the fretting corrosion less significant compared with tin-plating.

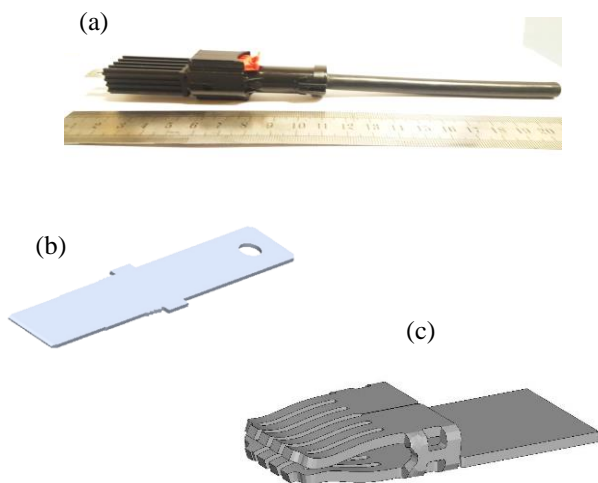


Fig. 2. (a) Automotive connector, (b) Pin, (c) Clip

## III. FE MODELING AND VIBRATION SIMULATION

The principle of the numerical modeling is shown in Fig. 3. It is based on a full 3-D FEA connector model (all the parts of connector, including the cable) by using LS-DYNA mechanical simulation software. The mechanical analysis consists in calculating the micro-displacements at each contact interface.

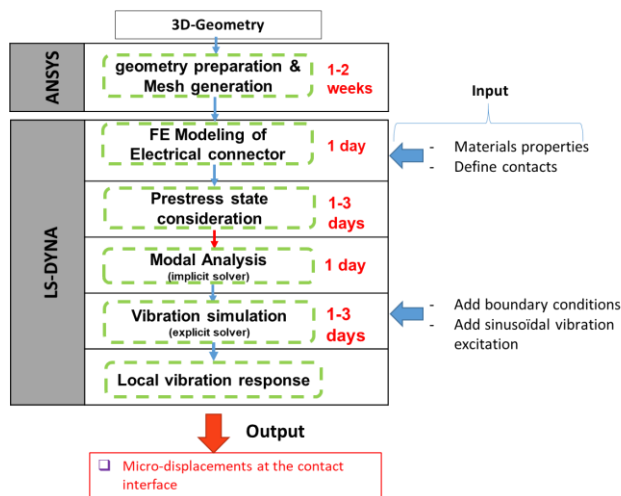


Fig. 3. Modeling and vibration simulation process

The FE modeling approach is divided into different steps before running vibration simulation:

### A. Step 1: Mesh generation & FE modeling

For the 3-D vibration analysis, the 3-D solid elements are used for the entire connector component. The mesh type generated is hexahedral as observed in Fig. 4. It is necessary for this connector model to refine the size and type of the mesh element in contact area so that the simulation results will be more accurate for the relative motions at the contact interface as shown in Fig. 5.

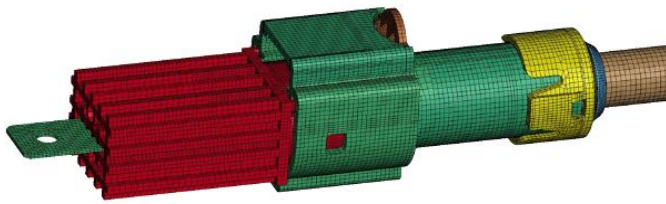


Fig. 4. 3-D model of automotive electrical connector

LS-DYNA keyword deck by LS-PrePost



Fig. 5. Modeling of the pin and clip after pairing up

This type of modeling of electrical connectors, leads to models of more reasonable size and more consistent with the explicit analysis carried out, but in return requires a greater investment in preparation time. The material properties (such as Young's modulus, Poisson's ratio and density) and the mechanical behavior are listed in Table I.

Table I. MATERIALS PROPERTIES

parts	Mechanical behavior	Thickness (mm)	Density (Kg.m <sup>-3</sup> )	E (GPa)	Poisson's ratio
Male housing	Elastic	-	1470	2.7 - 9.2	0.4
Female housing	Elastic	-	1470	2.7 - 9.2	0.40
Male terminal	Linear Plasticity	1	8819	125 - 130	0.35
Female terminal	Linear Plasticity	0.5	8819	125 - 130	0.35
Cable (145 mm)	Orthotropic elastic	-	4157	$E_t=8 - 50$ $E_f= 0,3 - 10$	$\nu_t=0.35$ $\nu_f=0.033$
Seals	Elastic	-	1000	1 - 3	0.496

The micro motion at the contact point is not the same nature than the motions in the rest of the connector: it is not described by the usual laws of mathematics used in simulation software. Furthermore, the motion at the contact point results in the interface modifications, and those modifications have an effect on the motion. Thus, the approach used for this simulation was to roughly model the contact area through the macroscopic coefficient of friction. In that case, the problem related to the simulation tool is simplified. Hence, taking into account the static and dynamic coefficient of friction is necessary in order to get closer to the physical phenomenon encountered at the interface between two moving contacts. The Table II shows the input static and dynamic coefficient of friction.

Table II. MATERIALS PROPERTIES

Materials	Static coefficient of friction	Dynamic coefficient of friction
Metal/Metal	0.15 - 1.6	0.058 - 0.084
Plastic/Metal	0 - 0.78	0 - 0.25
Plastic/Plastic	0.05 - 0.30	0.04

These simulations are very complex because they involve a large number of components. Indeed, the connector components are of different mechanical natures (metals, plastics, silicone materials and cables) and are in motion or interaction with respect to each other. Such systems also involve a very large number of frictional contacts (non-linear contacts) which are difficult to manage in simulation. Three types of mechanical contacts are used according to the connector design by using LS DYNA software: *Tied contact*, *Surface to surface contact* and *Automatic general contact*.

#### A.1. FE modeling of the cable

The Cable is an essential component in the connector. It allows the transmission of electrical energy to the terminals. The cable consists of twisted copper strands and coated with silicon insulator. The cable's cross section is 35 mm<sup>2</sup>. It is necessary to take into account representative cable properties in the modeling while keeping a reasonable model size of the connector system. In this case, the cable was modeled as a 3-D solid element as see in Fig. 6. Indeed, we assumed that the mechanical behavior is orthotropic elastic for small deformations. For such behavior, four parameters need to be assessed:

$E_t$ : Tensile Young modulus

$E_f$ : Flexural Young modulus

$\nu_t$  and  $\nu_f$ : primary and secondary Poisson's ratios respectively.

The bending and tensile tests were done in order to get the input parameters necessary for modeling the cable (see Table I). Then the cable behavior can be more faithfully reproduced.

LS-DYNA keyword deck by LS-PrePost

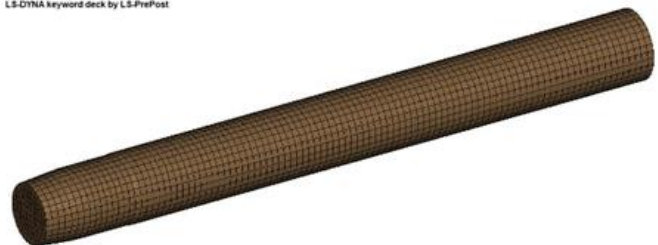


Fig. 6. Modeling of the cable as solid beam

#### A.2. Damping factor characteristics

The damping parameters of the connector components significantly influence their vibration amplitudes. In fact, the damping characteristics of cable majorly influence the motion

of the terminal connected thereto. In previous paper [17] we concluded that the motions were transferred from the cable to terminals parts. In this study, the influence of the damping ratio vs the relative motion at contact point was investigated. The global damping ratio used as input parameters in the FE model is between 2 and 5 %.

### B. Step 2: Prestress state consideration of terminals

This step consists of eliminating the initial interpenetration and tolerances between components due the mesh and make them pre-stressed (Fig. 7). The aim of this analysis is to obtain the prestress state mainly at the level of the metallic part of the contact. This state, due to the squeezing of the male part between the two lips of the female contact, sometime gives stress levels close (even locally higher) to the yield stress. The consideration of the initial prestress is mandatory in order to have realistic results. Furthermore, this setup also serves as the initial state for transient dynamic simulations.

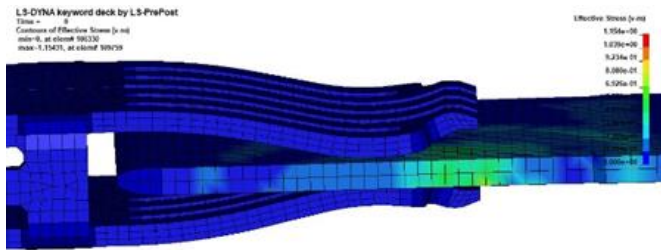


Fig. 7. Effective stress of electrical contact after prestress state consideration

### C. Step 3: Boundaries conditions

In the FE model and mechanical simulation of electrical connector, the boundary condition was displacements. The fixed constraint is a condition that allows to eliminate degrees of freedom, especially the translation motion. In this case, the fixed constraint was applied both at the end of the cable and the male housing (see in Fig. 8) in accordance with the physical configuration of the experimental test setup. The reason being that this fixation configuration is required by the automotive manufacturer standards as described in [5] - [7].

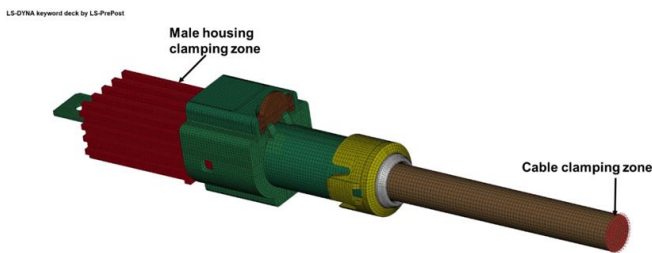


Fig. 8. Boundary conditions

### D. Step 4: Vibration simulation

Before vibration analysis, modal analysis is necessary in order to obtain the natural frequency of the electrical connector and this was done in previous study [17]. In the present paper, we only focused on non-resonate frequencies. For understanding the dynamical behavior of the terminals, the sinusoidal vibration simulation of electrical connector was added to the FE model (Fig. 9). The vibration was applied at the end of the cable and the male housing. The simulation was done at each three directions: Lateral (parallel (//) to X-axis), Axial (// Y-axis) and Vertical (//Z-axis). For a given direction of excitation, the displacements were calculated along 3 axes. In addition to the motions calculated according to the direction of excitation, this methodology also makes it possible to take into account the contribution of the orthogonal motions to the direction of excitation by using (5). The vibration motion that causes fretting damage is known as an explicit non-linear dynamic problem in the finite element field [15], so the LS-DYNA software with an explicit solver was used. The simulation is solved in the time domain. The calculation time depends on the frequency level applied. The calculation is carried out between 1-10 periods with a gradual rise over the first 2 periods of the sinusoidal profile to avoid a shock effect at start-up. After passing the calculations, we can clearly see a stabilization of the behavior from around the 3rd period.

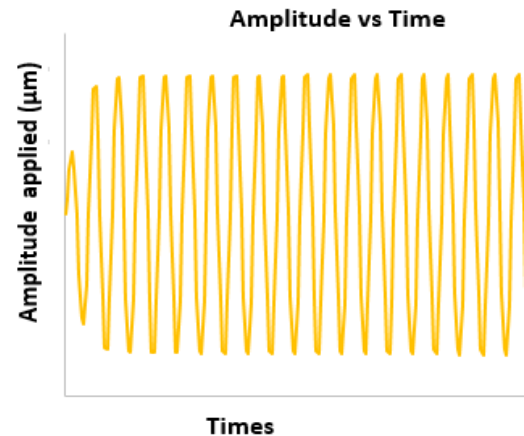


Fig. 9. Example of sinusoidal profile applied

The vibration conditions are applied for generating the fretting motion in contact point. The frequencies and accelerations are fixed at (200 Hz, 15 G) and (100 Hz, 10 G). The corresponding displacement amplitude ( $\delta^*$ ), calculated by using (1), are listed in Table III. These vibration conditions applied are close to those encountered in automotive standards.

The 3-D dynamic FE simulation is a time-consuming that requires many computing resources. However, only a few cycles of the vibrating motion can give a clear view of the relative motion. The Table III lists the input conditions for vibration.

$$\delta^* = \frac{a_m}{4\pi^2 f^2} \quad (1)$$

where  $a_m$  and  $f$  are the acceleration amplitude and the frequency respectively.

Table. III. Input excitation parameters

Conditions	Frequency	Acceleration	Displacement (peak-peak)
C1	200 Hz	15 G	185 $\mu\text{m}$
C2	100 Hz	10 G	497 $\mu\text{m}$

#### IV. EXPERIMENTAL CONFIGURATION

In order to validate the developed FE simulation model, a vibration bench test was built and set up with the aim to be as close as possible to the automotive vibrations environments conditions. The input vibration excitation is produced by using the LDS V555 shaker driven by an accelerometer. A schematic diagram of the experimental test setup is shown in Fig. 10. A sample holder, on which the connector is mounted, was especially designed and then rigidly fixed on the shaker head as displayed in Fig. 11-13. The connector fixed on the sample holder is in testing setup equipped with the male and female housings and a cable length of 145 mm.

The male housing was fixed to limit his movement in two directions perpendicular to electrical contact insertion. Furthermore, the cable was clamped. This fixing configuration ensures that the connector system follows the motion of the shaker head. In fact, the mounting apparatus was designed and secured in order to minimize added effects, i.e., harmonics, damping, resonances, etc.

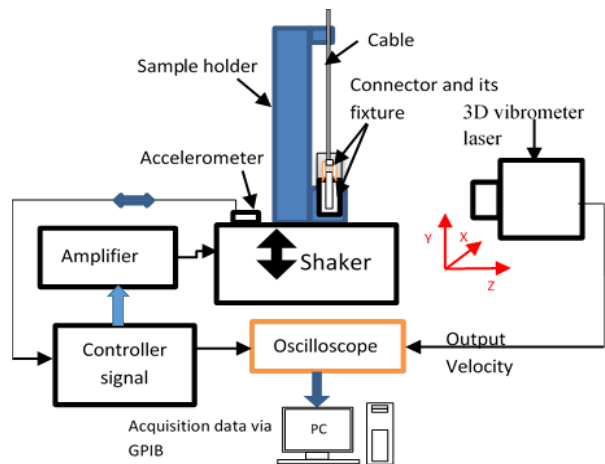


Fig. 10. A schematic diagram of the experimental test setup

This fixation configuration is required by the automotive manufacturer in accordance with the standard described in [5]-[7]. For a given connector sample, the vibration is applied along three directions with respect to the running order of each excitation's directions: 1<sup>st</sup>: Axial direction (// Y-axis) Fig. 11; 2<sup>nd</sup>: Lateral direction (// X-axis) as see in Fig. 12; and 3<sup>rd</sup>: Vertical direction (// Z-axis) as shown in Fig. 13.

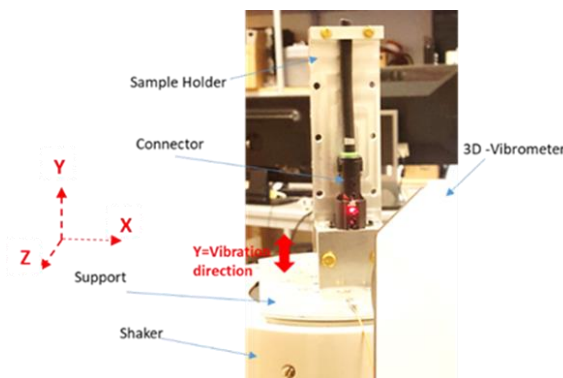


Fig. 11. Axial excitation (parallel to Y-axis)



Fig. 12. Lateral excitation (parallel to X-axis)



Fig. 13. Vertical excitation (parallel to Z-axis)

The parts inside the plastic housing (the male and female terminals) are accessible by making a hole around 5 mm of diameter, small enough in order to avoid modification of the mechanical proprieties of the connector [2].

A series of experiments tests were done to investigate mechanical behavior of automotive connectors subjected to vibration excitation. For a given direction of vibration excitation, the displacements are measured at each spatial axis. A LabVIEW acquisition data program has been developed on a computer to collect data from oscilloscope via GPIB cable. The vibrometer output is an analog voltage signal which describes the motion amplitude of the object.

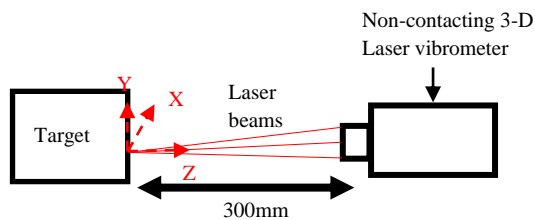


Fig. 14. Principle of Measurement geometry by using CLV 3-D laser vibrometer

### A. Measurement of Displacements

The displacement measurements of the different samples are carried out using Polytec 3-D laser Vibrometer that use reflecting a laser beam on a specified target surface. This equipment allows for measuring simultaneously, at a single-point targeted, all three linear velocity components of a vibrating structure (Fig. 14). The velocity resolution is between 0.5-1  $\mu\text{m/s}$  in a 10 Hz resolution bandwidth. The output is proportional to voltage signal, which describes the velocity of the object [24].

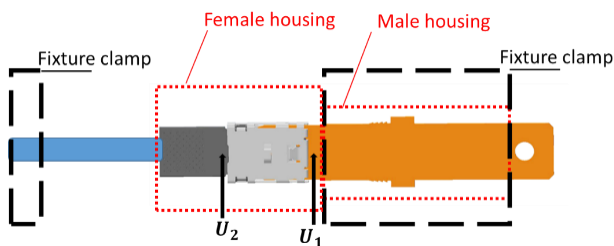


Fig. 15. Locations of measuring relative displacement

The Fig. 15 shows the measuring locations of the male and female parts through the hole. These 5 mm of diameter holes realized through the plastic housings allow to target the terminals under vibration. The displacement measurements of the different parts are deduced by integrating the velocity measured by the Vibrometer. The functions of the motions of the two spots are defined as  $U_1$  and  $U_2$ . For vibration applied in each direction, the maximum amplitudes of the sample holder, female housing, female terminal, male terminal and the cable were measured in 3-axes. We assume that the motion of the sample holder is the reference movement with respect to the amplitudes of the other components motions.

### B. Measured Relative displacement

The fretting corrosion damage is governed by the relative displacement of the contact pairs. Ideally, the relative displacement between two contact points should be measured simultaneously, but this requires duplicating expensive equipment (one 3-D laser vibrometer per piece). Our experimental set-up consists of only one 3-D laser Vibrometer. This causes a phase's determination problem between two measurement points. To solve this issue, we used the signal phase of the accelerometer as our reference point and we corrected our signal accordingly:

- i. By subtracting the reference phase from the phase of the measured signal
- ii. Then we will hence extract from previous measurements the relative displacements of the male part with respect to the female part as described by using (2), (3) [25].

The motions of the two parts can be approximated as sinusoidal functions:

$$U_1 = M_1 \sin(\omega t + \psi_1) \text{ for part 1} \quad (2)$$

$$U_2 = M_2 \sin(\omega t + \psi_2) \text{ for part 2} \quad (3)$$

Where  $M_1$  and  $M_2$  are the magnitudes and  $\psi_1$  and  $\psi_2$  are the phase shifts. The maximum relative displacement  $|\Delta\delta_{ij}|$ , along a given direction and axis, is defined as the modulus of the difference of  $U_1$  and  $U_2$ , which can be expressed as follows:

$$|\Delta\delta_{ij}| = |U_2 - U_1| = M_1 \sqrt{(1 - M \cos(\psi))^2 + (1 - M \sin(\psi))^2} \quad (4)$$

where  $M$  is the magnitude ratio,  $M_2/M_1$ , and  $\psi$  is the phase difference  $\psi_2 - \psi_1$ . The index "i" represents the direction of excitation (such as Axial, Lateral or Vertical) and "j" represents the axis of displacement measurement (X, Y, Z). As the 3-D Vibrometer laser measured the data in three axes simultaneously, the relative displacement in the total direction can be calculated by using (5), which allows to take into account the contribution of all the motions orthogonal to the input excitation direction.

$$||\Delta\delta_i|| = \sqrt{||\Delta\delta_{iX}||^2 + ||\Delta\delta_{iY}||^2 + ||\Delta\delta_{iZ}||^2} \quad (5)$$

## V. CONTACT RESISTANCE MEASUREMENTS

### A. Electrical endurance test on terminals

The relative motion of the contact interface induced by engine vibrations is one of the most significant causes for the fretting degradation. In order to determine the electrical endurance of the connector and the threshold amplitude of fretting corrosion, a series of tests were carried out on terminals only without the housings. The reason being that it is easier to control the relative motion by testing only the terminals instead of all the entire connector system. The male terminal of an electrical connector is submitted to vibration, whereas the female terminal is firmly attached to a fixed support, as shown in Fig. 16.

Electrical contact resistance during the test was measured using a 4-wire method [26]. The terminals are subjected to vibrations on the axial direction (in the insertion and extraction direction). The frequency is fixed at 100 Hz, which allows to accelerate the tests durabilities. The test is carried out with several amplitudes ( $\delta^*$ ) of displacement: from 20  $\mu\text{m}$  to 740  $\mu\text{m}$  peak to peak. The test duration was 48 hours, which correspond to 17  $10^6$  cycles without any increase of the electrical contact resistance.

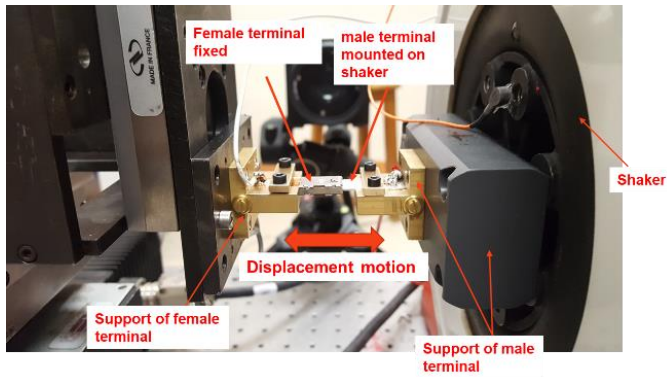


Fig. 16. Electrical endurance test device

A current source applies  $I = 100$  mA with limiting the voltage to 10 V while a Keithley  $\mu$ voltmeter measures the contact voltage with  $0.1 \mu\text{V}$  resolution. The number of fretting cycles ( $N_c$ ) to reach an electrical resistance threshold of  $\Delta R_c = 1\text{m}\Omega$  was taken as the lifetime of the electrical contact resistance (Fig. 17) [5].

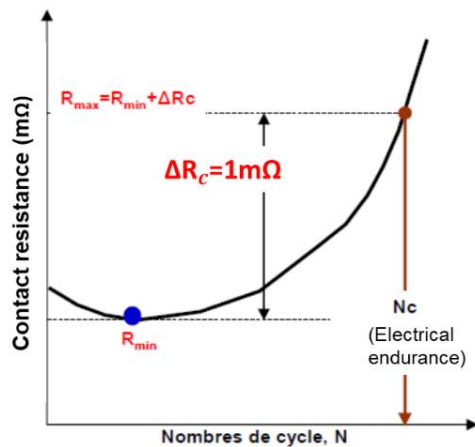


Fig. 17. Criterion used to identify electrical endurance  $N_c$

### B. Vibration test on connector system

In order to confirm the prediction methodology of fretting damage risk, the samples connectors were tested. The vibration with higher amplitudes and over longer periods of time, are applied to the connector in order to observe more degradation on the contact surface. The vibrations conditions are the same than listed in Table III and the test duration was 24 hours per axis. The fixture system used is the same that observed in Fig. 11, 12 and 13 with the cables connected on the power supply which is able to provide a DC current as high as 100 mA. As output, we measured the variation of the ECR. Finally, for each excitation direction, two connectors were submitted to vibration.

## VI. RESULT AND DISCUSSIONS

### VII.1. Vibration response with Fixed Amplitude and Frequency

The vibration profile was applied during this study allowed a good understanding of the dynamical response. The sinusoidal excitation with a single frequency and a constant amplitude was applied for the FE simulation and experimental test. In order to measure and calculate the relative displacement at contact point, two input conditions (C1 and C2) are used as described in the Table III. Both simulation and test motions results are plotted as a function of time, shown in Fig. 18 and Fig. 19. The relative displacement between the male (pin) and the female (clip) terminals is obtained by the subtraction of the pin motion and the clip motion so called "difference". The vibration motion computed with simulation agreed with the experimental results (Fig 19 and 18).

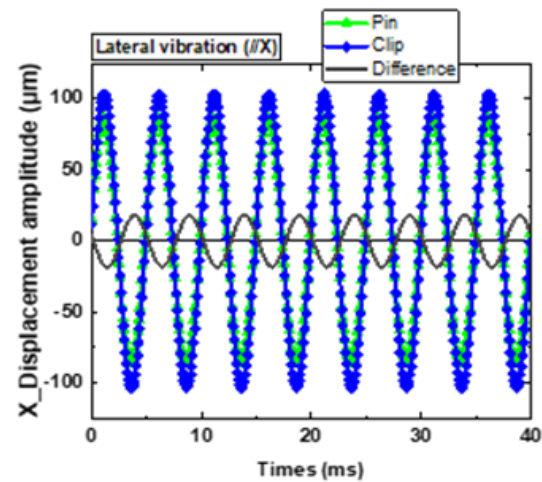


Fig. 18. Experiment results: Vibration applied at lateral direction and the motions measured along X-axis (200 Hz, displacement applied  $185 \mu\text{m}$  (peak-peak))

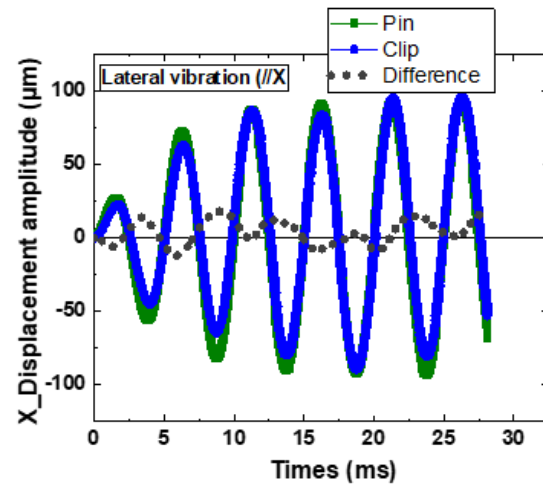


Fig. 19. Simulation results: Vibration applied at lateral direction and the motions measured along X-axis (200 Hz, displacement applied  $185 \mu\text{m}$  (peak-peak))

As shown on the Fig. 18 and 19 regarding the difference of motion between clip and pin, these curves of displacement difference between terminals have the same allure and the peaks of amplitude are close for both case the test and simulation analysis.

Actually,  $|U_2 - U_1|$  is an only rough approximation of the relative displacement between male and female parts at the contact surfaces because  $U_2$  is away from the contact surface of female part. Before to calculate the relative motion at contact interface, we verified the distribution of the motions of the female terminal at each node with FE simulation. We detected that the value of the displacement amplitude was the same for each node of the female terminal. This outcome is due to the mechanical behaviour of the female terminal. These results allow us to be more consistent with the following on the analysis of relative displacement at the contact interface. The detailed relative motion values and the responding frequencies applied are listed in Tables IV and V.

Table. IV. Simulation result for 200 Hz and 185  $\mu\text{m}$  (pk-pk)

Simulation results		Excitation direction		
		Lateral (L)	Axial (A)	Vertical (V)
Relative displacement at contact point $ \Delta\delta_{ij} $ ( $\mu\text{m}$ )	X	30	4	5
	Y	4	1	5
	Z	18	4	40

Table. V. Experiment test result for 200 Hz and 185  $\mu\text{m}$  (pk-pk)

Test results		Excitation direction		
		Lateral	Axial	Vertical
Relative displacement at contact point $ \Delta\delta_{ij} $ ( $\mu\text{m}$ )	X	27	2	No harmonic motion
	Y	5	3	17
	Z	3	5	52

Regarding the vibration at 200 Hz with a displacement applied 185  $\mu\text{m}$  (peak-peak) and fixed acceleration 15 G. The excitation was applied along the three directions (lateral, axial and vertical) and then measured and calculated in the corresponding three axes. The results of relative displacement at contact interface between the simulation and test seem to be close, except for  $\Delta\delta_{LZ}$  and  $\Delta\delta_{VZ}$  (seen in Table. IV and V). This low relative displacement observed for  $\Delta\delta_{LZ}$  and  $\Delta\delta_{VZ}$  in simulation is due to the type of mechanical contact defined between the male housing and the pin. Therefore, the male housing is fixed along the Z axis and transfer very low motion to the male terminal during lateral vibrations.

The difference detected for  $\Delta\delta_{VZ}$  is due to the large influence of the cable behavior.

Another comparison was done for the results at 100 Hz with a displacement applied 497  $\mu\text{m}$  (peak-peak). The results of the relative displacement are presented in Table VI and VII. We can observe that the magnitude of the relative displacements is similar for both test and simulation. In fact, a huge difference is detected for  $\Delta\delta_{LY}$ . Indeed, the differences observed between the simulation and the test about the values of the relative displacements might be caused by several factors such as the properties of the cable, the value of the damping factor taken into account, and the surface roughness. Firstly, some parameters are taken into account indirectly as input data (i.e. derived from the 3-D geometry of the connector). Secondly, certain parameters are considered directly as input data (view Table I and II). In addition, the difference between the dimensions of the real connector and the CAD geometry can influence a priori the motion mappings of the different components in interaction with each other.

Table. VI. Simulation result for 100 Hz and 497  $\mu\text{m}$  (pk-pk)

Simulation results		Excitation direction		
		Lateral	Axial	Vertical
Relative displacement at contact point $ \Delta\delta_{ij} $ ( $\mu\text{m}$ )	X	62	12	9
	Y	49	22	No harmonic motion
	Z	11	5	58

Table. VII. Experiment test result for 100 Hz and 497  $\mu\text{m}$  (pk-pk)

Test results		Excitation direction		
		Lateral	Axial	Vertical
Relative displacement at contact point $ \Delta\delta_{ij} $ ( $\mu\text{m}$ )	X	70	14	6
	Y	35	18	No harmonic motion
	Z	No harmonic motion	1	43

Indeed, low motions of non-harmonic were observed in the lateral direction for  $\Delta\delta_{LZ}$  and the vertical direction for  $\Delta\delta_{VZ}$ . The movements measured at the terminals were not sinusoidal. It was sometimes a non-harmonic signal due to a shock between the components, on the one hand. On the other hand, some non-harmonic signals measured were simple noises. We have therefore chosen to not take them into account.

From previous results, the relative displacement in the total direction  $|\Delta\delta_{ij}|$  was calculated by using (5). The comparison between simulation and test results regarding the  $|\Delta\delta_{ij}|$  is shown in Fig. 20 and 21.

These results are determined at C1 and C2 conditions. We can observe that the simulation results are close to the test. The relative motions observed in Axial direction are less than those obtained along lateral and vertical vibration directions. This is due to the cable soft behavior under vibration excitation. The cable undergoes both bending and tension movement combined under vibration. Along lateral and vertical direction, the cable presents the bending motions which allow the important displacement to the connector components. The relative displacement between terminals in the total direction  $\|\Delta\delta_t\|$  is an important parameter which will be used in the following to predict the risk of the fretting apparition at contact point.

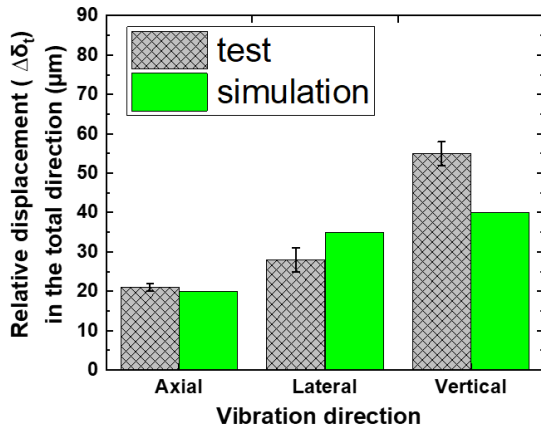


Fig. 20. The relative displacement between terminals in the total direction of excitation (200 Hz and 185 μm (pk-pk))

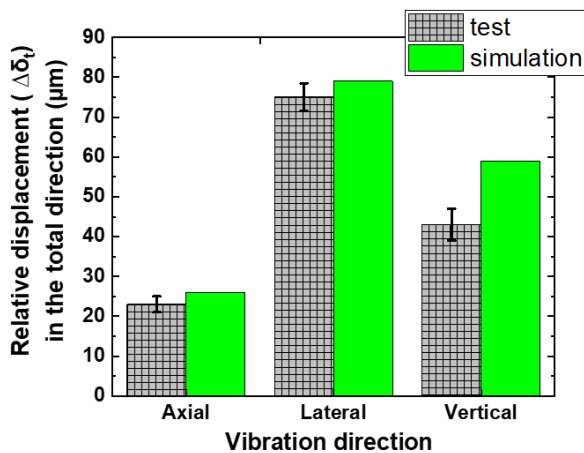


Fig. 21 The relative displacement between terminals in the total direction of excitation (100 Hz and 497 μm (pk-pk))

## VII.2. Electrical endurance results

In the previous part, we determined the relative motions at contact point when all the connector system is subjected to sinusoidal vibration. Thus, the second step in our approach to predict the vibration performance of the electrical connector consists in characterizing its electrical endurance, especially, to determine the threshold amplitude ( $\delta_{Limit}$ ) and the critical number of cycle ( $N_c^*$ ) of fretting degradation.

In this experiment, testing was performed on clip/pin terminals only, without the plastic housings. The male contact is subjected to a high number of vibrations while the female contact is firmly attached to a fixed support (see Fig. 16). The fretting tests were performed for different displacement amplitudes and the critical number of cycle ( $N_c^*$ ) has been reported for each test in Table VIII.  $N_c^*$  is defined as the number of cycles necessary to reach a threshold of  $\Delta R_c = 1 \text{ m}\Omega$ , from which it is considered that there is a break of a good electrical conduction.

Table. VIII. Quantitative data related to the electrical endurance

$\delta^*(\pm\mu\text{m})$	Electrical endurance $N_c$	
	test 1	test 2
20	>17 280 000 <sup>c</sup>	>17 280 000 <sup>c</sup>
30		
38		
40		
50		
70		
90	5 670 000	5 850 000
120	2 240 000	2 641 000
160	2 010 000	1 889 000
220	3 334 000	
250	1 390 000	
350	895300	
500	637300	
740	400 000	

<sup>c</sup> Test stopped without failure

From Fig. 22 being a graphical presentation of data from Table VIII, it can be observed that, lifetime of electrical contact (number of cycles  $N_c$ ) decreases together with the increase of displacement amplitude which goes in line with the results [4], [22].

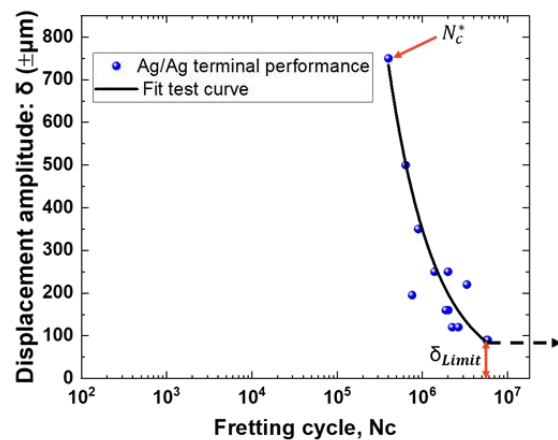


Fig. 22. Evolution of electrical contact resistance after fretting test

From the electrical endurance test, we detected a threshold displacement amplitude ( $\delta_{Limit}$ ) around  $\pm 90 \mu\text{m}$ . And, from both simulation and experiment test of vibration, we determined the relative displacement at contact point in the total direction  $\|\Delta\delta_t\|$ . This mechanical parameter associated to

the threshold displacement amplitude ( $\delta_{Limit}$ ) can conveniently be considered as the pertinent criterion to predict a low and stable electrical contact resistance:

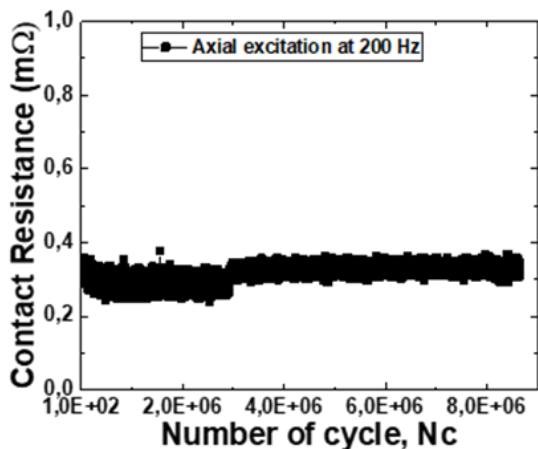
If  $\|\Delta\delta_i\| > \delta_{Limit}$ ,  $\Delta R_c$  increases, the electrical contact endurance displays a finite lifetime.

If  $\|\Delta\delta_i\| < \delta_{Limit}$ ,  $N_c \rightarrow \infty$ ,  $\Delta R_c$  low and stable, the electrical contact endurance displays an infinite endurance.

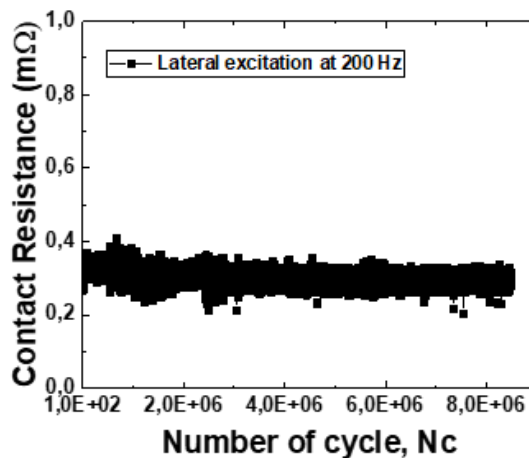
The relative displacement at contact point in the total direction  $\|\Delta\delta_i\|$ , calculated from simulation and test results are less than the ( $\delta_{Limit}$ ). We assumed that for the conditions presented on table III, there is no risk of connector degradation because  $\Delta R_c$  will remain low and stable. The samples connectors tested present the good performance under vibration conditions applied.

### VII.3. Confirmation of the predictive model approach

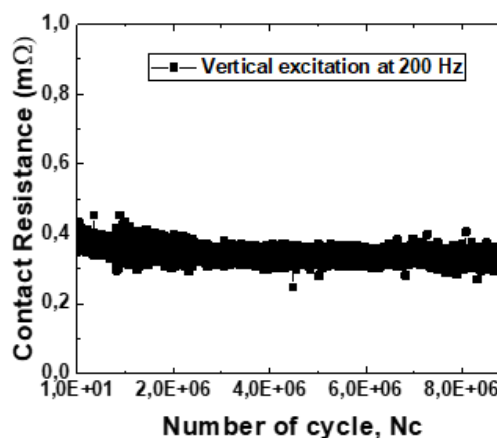
In order to confirm the prediction methodology proposed in this study, the entire electrical connector system was submitted on vibrations with higher amplitudes and over longer periods (24 hours) per axis. Fig. 23 shows the evolution of the connector ECR measured under vibration at (200 Hz, 185  $\mu\text{m}$ ) and (100 Hz, 497  $\mu\text{m}$ ). The ECR measurement is performed by the 4-wire method. For each connector sample tested, the recording of electrical contact resistance data was one measurement every 4 seconds. No micro cuts were observed throughout the duration of the various tests carried out. The contact resistance remains stable (seen Fig. 23) regarding the conditions applied in Table I. The prediction approach using experiment and simulation results were very conclusive and confirmed the finite element models developed for high vibration simulation.



(a)



(b)



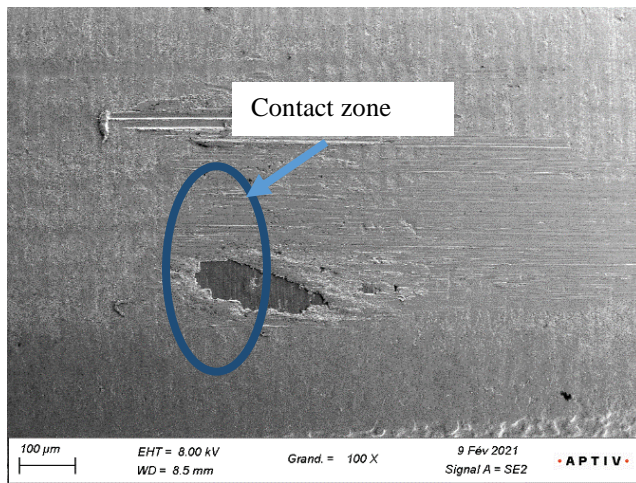
(c)

Fig. 23. Evolution of electrical resistance at 200Hz, 185  $\mu\text{m}$  (peak-peak), (a) Axial excitation, (b) Lateral excitation, (c) vertical excitation

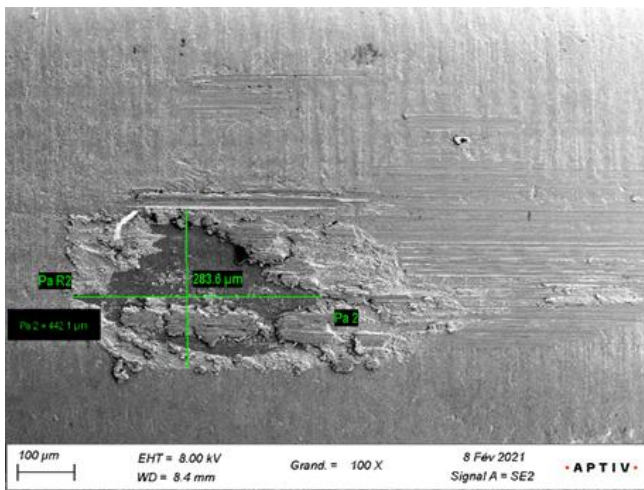
As observed in Fig. 23 (a), 23(b) and 23 (c), at the start of the test the  $R_c$  decreases slightly which corresponds to a flattening of the contact surface and thereafter it increases slightly and remains almost weak and stable. In fact, the displacement relative at contact point does not pass the threshold amplitude, until the end of the fretting cycle for such conditions. This confirms the predictive approach proposed.

### VII.4. Wear analysis after vibration

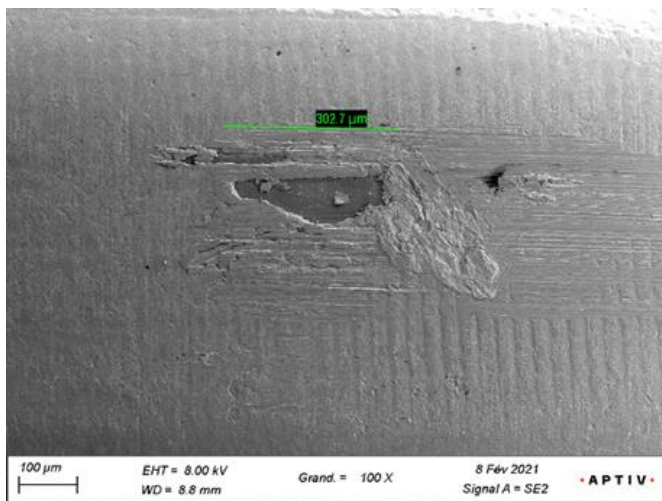
The surfaces of the power connectors are plated with silver over a bulk material of copper. After testing vibrations are applied to the whole connectors, an inspection of surfaces was done in order to analyze if wear and corrosion may occur. In order to study the effects of vibration on the surface wear of the connectors, scanning electron microscopy (SEM) is taken from a worn contact surface of the female terminal after a vibration test. Since the contact resistance does not increase during vibration test over the longer, as shown in Fig. 24, the wear and corrosion on the contact surface may be insignificant.



(a)



(b)



(c)

Fig. 24 SEM on worn contact surface of terminal female after vibration test at 200Hz, 185  $\mu\text{m}$  (peak-peak), (a) Axial excitation, (b) Lateral excitation, (c) vertical excitation.

The results in Fig. 24 (a), (b) and (c) show that vibrations have caused some wear and little fretting wear. For twelve clip's contact zones analyzed, only slight wears were observed on certain portions of the contact zone. These wears on a certain small parts of contact zone are explained by the fact that the distribution of the contact force is not uniform over each contact point, on one hand. On the other hand, the fact of observing wear on a portion of the contact zone suggests that the pin is not perfectly aligned when it is inserted and pinched inside the clip. In addition, the analysis shows that the defect area on the surface can be referred as a worn pit rather than corrosion because the main finding is indentation and removal of coating material. If fretting corrosion occurs, there would be material accumulation and a more random appearance in the SEM image [11]. Finally, the silver coating that is resistant to oxidation in the air, the wear particles could not increase the contact resistivity and the electrical contact resistance will not gradually increase under vibration.

## VII. CONCLUSIONS

Fretting corrosion damage is caused by a relative motion of contact pairs surfaces, submitted to external mechanical vibrations. A highly detailed 3-D FEA model for an automotive electrical connector has been developed and analyzed to explore the relative motion between the contacts male/female under vibration conditions. A series of experiments test was also conducted to validate and test the simulation. The LS DYNA explicit technique was used in order to perform simulation. This study's findings can be summarized and concluded as follows:

- 1) The relative motion values of contact pairs were measured for different single excitation frequencies in both experiment and simulation. Results from the simulations generally matched that from the corresponding experiments quite well. The deformation of the cable produced motion orthogonal to the input excitation direction.
- 2) This paper studied the electrical performance and fretting mechanism of silver-plated power connectors subject to different vibrations. Firstly, the terminals endurance were investigated in order to determine the threshold fretting amplitudes. Secondly, the ECR of the connectors was measured to assess the effects of the conditions on performance.
- 3) The prediction methodology of the fretting degradation, based on experiment and test results, was proposed in this paper. Then a good confirmation of this predictive methodology was established and validated.
- 4) The present FE modeling and analysis have demonstrated a good potential for evaluating the dynamic behavior of electrical connector under vibration.

Suggested further research includes the calculation of the relative motion transfer functions at contact interface. In

addition, the prediction approach of fretting damage will be proved and extrapolated using an automotive vibration profile.

## REFERENCES

- [1] A. Bouzera, E. Carvou, N. Ben Jemaa, R. El Abdi, L. Tristani, and E.M. Zindine. Minimum fretting amplitude in medium force for connector coated material and pure material. 56th IEEE Holm Conference on Electrical Contacts, pages 101–107, 2010.
- [2] J Labbé, "Détection et étude de microdéplacement des contacts sous contrainte vibratoire et leurs conséquences sur les matériaux et revêtements des connecteurs automobiles", Phd thesis, Rennes, 2017.
- [3] S. E. Mossouess et al., "Analysis of temporal and spatial contact voltage fluctuation during fretting in automotive connectors," ICEC 2014; The 27th International Conference on Electrical Contacts, Dresden, Germany, 2014, pp. 1-5.
- [4] Fouvry S., Jędrzejczyk P., Chalandon P., Introduction of an exponential formulation to quantify the electrical endurance of micro-contacts enduring fretting wear: application to Sn, Ag and Au coatings, *Wear* 271, pp. 1524-1534, 2011.
- [5] LV 214-3 Motor Vehicle Connectors; Test Sequences, 2010.
- [6] PSA Peugeot-Citroën, "Connectors general requirements" Standard B217050.
- [7] Performance specification for automotive electrical connector systems SAE/USCAR, February 2013.
- [8] Chen Chen, George T. Flowers, Michael Bozack, and Jeffrey Suhling, "Modeling and analysis of a connector system for the prediction of vibration-induced fretting degradation," Proceedings of the 55th IEEE Holm Conference on Electrical Contacts, September 14-16, 2009, pp.131-137.
- [9] M. Varenberg, I. Etsion, and G. Halperin, "Slip index: A new unified approach to fretting," *Tribol. Lett.*, vol. 17, no. 3, pp. 569–573, 2004.
- [10] R. D. Ibrahim, C. Chen, and G. T. Flowers, "Modeling and analysis of a blade/receptacle pair for the prediction of thermal cycling and temperature dependent vibration driven fretting corrosion," in Proc. 56th IEEE Holm Conf. Electr. Contacts, Charleston, SC, USA, Oct. 2010, pp. 1–7.
- [11] N. Saka, M. J. Liou, and N. P. Suh, "The role of tribology in electrical contact phenomena," *Wear*, vol. 100, nos. 1–3, pp. 77–105, Dec. 1984.
- [12] L. Kogut and K. Komvopoulos, "Electrical contact resistance theory for conductive rough surfaces," *J. Appl. Phys.*, vol. 94, no. 5, pp. 3153–3162, Sep. 2003.
- [13] F. Ossart, S. Noel, D. Alamarguy, S. Correia, and P. Gendre, "Electromechanical modelling of multilayer contacts in electrical connectors," in Proc. 53rd IEEE Holm Conf. Electr. Contacts, Pittsburgh, PA, USA, Sep. 2007, pp. 1–8.
- [14] P. van Dijk, A. K. Rudolphi, and D. Klaffke, "Investigations on electrical contacts subjected to fretting motion," in Proc. 21st Int. Conf. Elect. Contacts, Zürich, Switzerland, 2002, pp. 9–12.
- [15] F. Zang, thesis, A Study of Vibration-induced Fretting Corrosion in Electrical Connectors Based on Experimental Test and FEA Simulation, Auburn, Alabama August 2, 2014
- [16] K. Mashimo, H. Katayama, H. Nishikubo, and Y. Ishimaru, "Influence of Vibration on Connector Sliding Mode and Amplitude," Proceedings of the 60th IEEE Holm Conference on Electric Contacts, pp. 289-296, October 12-15, 2014.
- [17] M. Mavuni, E. Carvou, G. Lalet, Study of vibration transfer in automotive connectors for understanding of fretting corrosion damage, ICEC, 2020.
- [18] Yahya, O. and Miled, H., "Modeling of the Impact of Ultrasonic Welding of Harness on the Terminals Integrity," SAE Technical Paper 2014-01-0224, 2014, <https://doi.org/10.4271/2014-01-0224>.
- [19] G. T. Flowers, F. Xie, M. Bozack, and R. Horvath, "Modeling early-stage fretting of electrical connectors subjected to random vibration," *IEEE Trans. Comp. Technol.*, vol. 28, no. 4, pp. 721–727, Dec. 2005.
- [20] F. Hubner-Obenland and J. Minuth, "A new test equipment for high dynamic real-time measuring of contact resistances," in Proc. 45th IEEE Holm Conf. Electr. Contacts, Pittsburgh, PA, Oct. 1999, pp. 193–202.
- [21] E. Carvou and N. B. Jemaa, "Time and level analysis of contact voltage intermitences induced by fretting in power connector," in Proc. 53rd IEEE Holm Conf. Electr. Contacts, Pittsburgh, PA, Sep. 2007, pp. 211–215.
- [22] F. Pompanon, J. Laporte, S. Fouvry, O. Alquier, "Normal force and displacement amplitude influences on silver-plated electrical contacts subjected to fretting wear: A basic friction energy – contact compliance formulation", *wear*, Volumes 426–427, Part A, 30 April 2019, Pages 652-661.
- [23] R. Fu, S. Choe, R. L. Jackson, G. T. Flowers, M. J. Bozack, L. Zhong, D. Kim, Vibration induced changes in the contact resistance of high-power electrical connectors for hybrid vehicles, *IEEE Transactions on Components, Packaging and Manufacturing Technology*, 2 (2) (2012), 185-193.
- [24] User Manual 3-D Laser Vibrometer CLV Polytec.
- [25] G. T. Flowers, Fei Xie, M. Bozack and R. D. Malucci, "Vibration thresholds for fretting corrosion in electrical connectors," Proceedings of the Forty-Eighth IEEE Holm Conference on Electrical Contacts, Orlando, FL, USA, 2002, pp. 133-139.
- [26] Holm. Electrical Contacts: theory and application. Springer - Verlag. Berlin 1967.



**Mack Mavuni Nzamba** was born in Kinshasa, Democratic Republic of Congo (DRC). He received the B.S. degree in materials engineering from National School of Engineering of Sfax, Sfax, Tunisia and the

M.S. degree in mechanical and materials engineering from the Ecole Nationale Supérieure des Arts et Métiers ENSAM-ParisTech, Paris, France, in 2015 and 2017 respectively. In 2022, he received the Ph.D. degree in mechanical engineering from Rennes University, Rennes, France. He worked as an Engineer R&D at APTIV company in France. He is currently an Associate Professor with the Department of Sciences Technology, University of Nouveaux Horizons, Lubumbashi, Democratic Republic of Congo. His research concerns the Multiphysics modeling and electrical connectors performances.



**Erwann CARVOU** received the Ph.D. degree in Electronics from the University of Rennes in 2003. Currently leading research group on electrical contacts in the institute of physic of Rennes. His research concerns the conduction and effect of arc disconnection on connectors.

**Laurent Morin**, received the the Ph.D in physics for engineering from the University of Rennes, France. He is an Engineering Manager with the Advanced Development Team, Aptiv, Epernon, France, with an organizational focus on the development of new connector.